Bone Reports 12 (2020) 100237

Contents lists available at ScienceDirect

Bone Reports

journal homepage: www.elsevier.com/locate/bonr

CXCR2 specific endocytosis of immunomodulatory peptide LL-37 in human monocytes and formation of LL-37 positive large vesicles in differentiated monoosteophils

Zhifang Zhang[a,*], Keith Le[a], Deirdre La Placa[a], Brian Armstrong[b], Marcia M. Miller[c], John E. Shively[a,*]

[a] Department of Molecular Immunology, Beckman Research Institute of City of Hope, 1500 E Duarte Road, Duarte, CA 9101, United States of America
[b] Light Microscopy Core, Beckman Research Institute of City of Hope, 1500 E Duarte Road, Duarte, CA 9101, United States of America
[c] Electron Microscopy Core, Beckman Research Institute of City of Hope, 1500 E Duarte Road, Duarte, CA 9101, United States of America

ARTICLE INFO

Keywords:
Monocytes
Monoosteophils
LL-37
Cathelicidin
Confocal microscopy
Electron microscopy

ABSTRACT

Immunomodulatory peptide cathelicidin/LL-37 induces human monocyte differentiation into a novel bone repair cell, the monoosteophil. We now demonstrate that LL-37 is endocytosed by monocytes over a period of 6 days producing large (10 × 2 μm), specialized LL-37 and integrin α3 positive vesicles. CXCR2, a membrane receptor previously associated with the binding of LL-37 to neutrophils, was co-endocytosed with LL-37 where both markers remained within the cytosol over a 16 h observation period. Endocytosis of LL-37 was mediated by a clathrin- and cavoelin/lipid raft-dependent pathway into early Rab5+ endosomes expressing APPL1 and EEA1. From 4 to 16 h, LL-37 vesicles co-localized with the Golgi, mitochondria, and to a lesser extent lysosomes and ER. By day 6, LL-37 was associated with large (> 10 μm) vesicles, adjacent to Golgi, mitochondria, ER and lysosomes. LL-37 co-stained with integrin α3, tetraspanin CD9, GPI-linked CD59 and costimulatory molecule CD276 (B7-H3) in these vesicles. Continuous tracking of LL-37 with its associated vesicles over 6 days indicates that LL-37 is an extremely stable, membrane-associated peptide that plays a critical role in the differentiation of monocytes into monoosteophils.

1. Introduction

Human cationic peptide LL-37, a proteolytic fragment of cathelicidin (hCAP-18), was first isolated in the specific granules of human neutrophils (Sorensen et al., 1997). In response to inflammation, LL-37 is produced by epithelial cells and many cells of the immune system (Vandamme et al., 2012; Hancock et al., 2016), including neutrophils (Sorensen et al., 1997), dendritic cells (Sigurdardottir et al., 2012), monocytes and macrophages (Sonawane et al., 2011; Rivas-Santiago et al., 2008). In addition to its antibacterial activity (Yang et al., 2004), LL-37 is a multifunctional modulator of innate immune responses (Scott et al., 2002), including protection of the urinary tract (Chromek et al., 2006), stimulation of angiogenesis (Koczulla et al., 2003), cutaneous wound-healing (Heilborn et al., 2003), chemoattraction of inflammatory and immune cells (Agerberth et al., 2000; De et al., 2000) and bone repair (Zhang and Shively, 2010; Zhang and Shively, 2013). In the case of activated neutrophils, the production of LL-37 leads to secondary necrosis (Zhang et al., 2008; Li et al., 2009; Bjorstad et al., 2009), a process identical to NETosis (Hoppenbrouwers et al., 2017).

In a previous study, we reported that a single treatment of human monocytes with LL-37 induced monocyte differentiation over a period of 6 days into a novel type of bone forming and bone repair cell termed the “monoosteophil”. When human monoosteophils were implanted in a freshly drilled hole in mid diaphyseal femurs of NOD/SCID mice, significant bone repair required only 14 days compared to 24 days for untreated controls (Zhang and Shively, 2013). Monoosteophils exhibit a gene expression signature distinct from mesenchymal stem cells, including proteins associated with both the osteoblast and osteoclast lineage (Zhang and Shively, 2013). Among the genes expressed, integrin α3 was a unique marker in that it was not expressed in monocytes treated with GM-CSF, M-CSF, or M-CSF plus RANKL, standard treatments for the differentiation of monocytes into other lineages. In those studies we did not examine the early stages of the uptake of LL-37 into monocytes, nor its fate after internalization.

We now report that LL-37 is endocytosed mainly through a clathrin- and caveolin/lipid raft-dependent pathway involving the early

* Corresponding authors.
E-mail addresses: jshively@coh.org (Z. Zhang), zzhang@coh.org (J.E. Shively).

https://doi.org/10.1016/j.bonr.2019.100237
Received 16 July 2019; Received in revised form 4 December 2019; Accepted 12 December 2019
Available online 13 December 2019

endosomal markers Rab5, APPL1 and EEA1. Treatment of monocytes with fluorescent labeled LL-37 triggers endocytosis of CXCR2, a receptor we previously reported for LL-37 on neutrophils (Zhang et al., 2009). Although LL-37 remains associated with only a portion of the CXCR2 positive endosomes, both LL-37 and CXCR2 marked endosomes remain largely undegraded in the cytosol over a period of 16 h. After initial endocytosis, LL-37 positive endosomes become associated with mitochondria and the Golgi apparatus. After 6 days, LL-37 is associated with large vesicles (10 × 2 μm). These membrane enclosed vesicles costain for LL-37 and integrin α3, a marker we previously associated with monoosteophils (Zhang and Shively, 2010)

2. Materials and methods

2.1. Antibodies and reagents

Antibodies to caveolin-1 (D46G3), clathrin HC (D3C6), Rab5 (C8B1), APPLI (D83H4), EEA1 (C45B10), Rab9A (D52G8), Rab11 (D4F5) and syntaxin-6 (C34B2) rabbit antibodies were from Cell Signaling Technology. MITO-ID Red, Golgi ID Green, ER ID Red and Lyso ID Red were purchased from Enzo Life Sciences. Anti-α3 integrin (CD49c) and APC-anti-α3 integrin (CD49c) antibody (clone ASC-1), anti-CD9 antibody and FITC anti-CD9 antibody (clone H19a), PE anti-human IGF-1R (clone 1H7/CD221), PE anti-human CD115 (clone 9-4D2-1E4), PE anti-human EGFR (AY13), anti-CD59 antibody and PE anti-CD59 antibody (p282), anti-CD276 antibody and APC anti-CD276 antibody (MIH42), anti-CCR2 antibody (K036C2) and anti-CXCR4 antibody (12G5) were from Biolegend. Anti-CXCR2 antibody and APC anti-CXCR2 (Clone 6C6) were from BD Biosciences. Anti-TIMP3 antibody was from Biorbyt Ltd. (Cambridge, United Kingdom). Alexa 555 goat anti-IgG H + L antibodies were from Life Technologies. Alexa 647 anti-P2Y11 (505214) and Alexa 647 anti-MRGX2 (477533) were from R &D Systems. Anti-human LL-37 antibody (1C12) was from Hycult Biotch. Goat anti-mouse IgG (H&L):15 nm Gold was from BBI Solutions. LL-37 was synthesized by the standard FMOC chemistry, purified by reversed phase HPLC, and the mass verified by nanospray mass spectrometry. The concentration was determined by amino acid analysis (Zhang et al., 2008).

2.2. Monocyte preparation and differentiation

Anonymous discard citrated blood without the requirement for informed consents was approved by the City of Hope IRB, IRB number 99132. PBMCs were isolated by Ficoll-Paque Plus density gradient centrifugation. Monocytes were isolated using EasySep Human Monocyte Enrichment Kit (StemCell Technologies). Monocytes (95% purity by Flow) were suspended at 1×10^6 cells/mL in αMEM medium supplemented with 10% FBS (< 5 pg/100 mL endotoxin) and treated with either 5 μM LL-37 or 5 μM LL-37-FAM (LL-37: LL-37-FAM = 4:1). For inhibition of LL-37-FAM endocytosis, monocytes were pretreated with Pitstop2 (Abcam) or Methyl-β-cyclodextran (Sigma-Aldrich) or both for 30 min, then treated with LL-37-FAM for 2 h.

2.3. Confocal immunofluorescence microscopy

Colocalization of LL-37-FAM with various markers was performed on monocytes that were fixed/permeabilized with eBioscience intracellular fixation & permeabilization buffer, and stained with primary antibodies for 30 min. After washing with PBS containing 1% BSA and 0.1% saponin, cells were stained with secondary Alexa 488 or 555 conjugated antibodies for 30 min. After washing, stained cells were mounted with Hard Set mounting medium with DAPI (Victor Laboratories, Inc., Burlingame, CA) and analyzed using a Carl Zeiss confocal laser scanning microscope. Quantification of colocalization of LL-37-FAM with other markers was analyzed using Pearson correlation coefficient using ImagePro Premier 9.2 software (Media Cybernetics, Inc., MD).

2.4. Transmission and immunoelectron microscopy

Cells were harvested and cryo-fixed in a Leica EM PACT2 high pressure (~2000 bars) as follows: cryo-fixed specimens were freeze-substituted in anhydrous acetone containing 0.5% glutaraldehyde and 0.1% uranyl acetate. The temperature progression was 48 h at −90 °C, −90 °C to −50 °C at 5 °C/h, −50 °C for 16 h. At −50 °C, the specimen was rinsed with acetone 3 times, 20 min each, and infiltrated with 50% Lowicryl H20 in acetone for 2 h, 67% Lowicryl H20 in acetone for 2 h, 100% Lowicyrl H20 overnight with two exchanges. Infiltrated specimen was polymerized in Lowicryl H20 for 24 h at −35 °C under a UV lamp and continued to polymerize at 25 °C for another 48 h. Ultra-thin sections (~70 nm thick) were cut using a Leica Ultra cut UCT ultramicrotome with a diamond knife on 200 mesh nickel EM grids. Grids were stained with 2% uranyl acetate in 70% ethanol for 1 min followed Reynold's lead citrate staining for 1 min. Post-embedding immunolabeling was carried out with anti-LL-37 antibody with 15-nm colloidal gold conjugated secondary antibody. The grids were imaged on a FEI Tecnai 12 transmission electron microscope equipped with a CCD camera.

2.5. Statistical analyses

Assay results are expressed as means ± SEM and statistics were calculated using GraphPad Prism 7.0 (San Diego, CA). Differences were analyzed by paired *t*-test and all *p* values are two-sided. Confocal MFI quantification was performed by the Pearson correlation coefficient using ImagePro Premier 9.2 software

3. Results and discussion

3.1. Endocytosis of LL-37

Since a single treatment of human monocytes with the peptide LL-37 is sufficient to induce the formation of the long lived bone repair cells called monoosteophils (Zhang and Shively, 2010), we were interested in determining the earliest events including receptor mediated uptake and the fate of the endocytosed LL-37. In order to follow LL-37 uptake at the cellular level we performed confocal microscopic analysis of fluorescent labeled LL-37 (LL-37-FAM) treated monocytes over 16 h. The concentration of LL-37-FAM (5 μM) that leads to differentiation of monocytes into monoosteophils, including prolonged survival, altered morphology and up-regulation of integrin α3 (Fig. S1) was similar to that previously reported for unlabeled LL-37 (Zhang and Shively, 2010). As shown in Fig. 1, LL-37-FAM was internalized at both the 1 h and 2 h time points into small vesicles in the cytosol. At the 4 and 16 h time points, the small vesicles merged into larger LL-37-FAM positive cytosolic vesicles with no evidence of nuclear accumulation. In contrast, it was reported that Texas Red labeled LL-37 was internalized by immature human dendritic cells into both the cytosol and nucleus (Bandholtz et al., 2006). Thus, the uptake and subcellular localization of fluorescently labeled LL-37 differs between fresh monocytes and DCs, another monocyte derived differentiated cell.

3.2. Co-endocytosis of CXCR2 with LL-37

CXCR2, a prominent chemokine receptor expressed on the cell surface of both neutrophils and monocytes, was previously found by us to serve as a receptor for LL-37 on human neutrophils (Zhang et al., 2009). In addition to our work, other studies have reported FPR2 (De et al., 2000), P2X7 (Elssner et al., 2004), P2Y11 (Brandenburg et al., 2010), MRGX2 (Subramanian et al., 2011), IGF1R (Girnita et al., 2012), EGFR (Yin and Yu, 2010), and Mac-1(Zhang et al., 2016) as LL-37 receptors on several types of cells. To examine potential LL-37 receptors

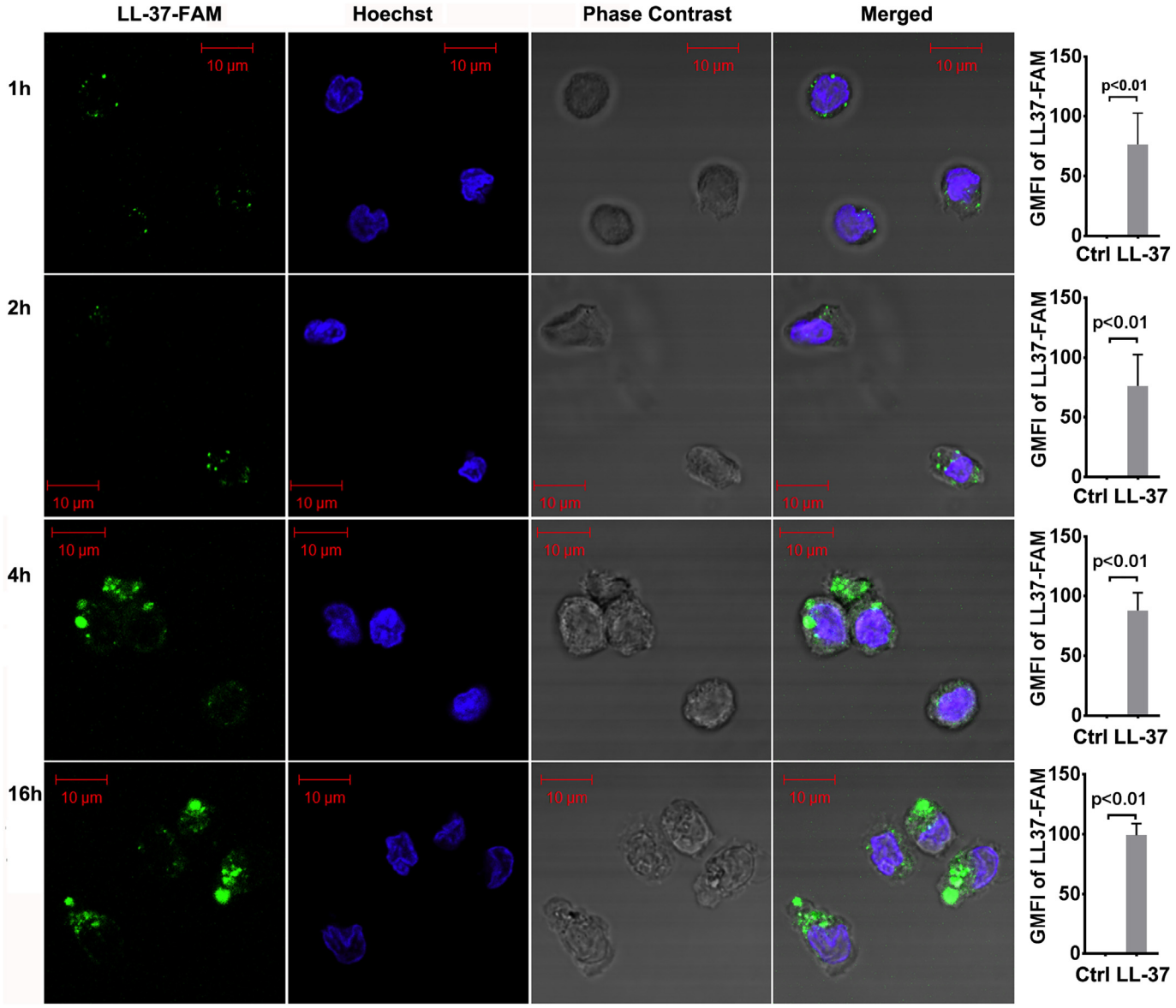

Fig. 1. Endocytosis of LL-37 of human monocytes. Human monocytes (1×10^6 cells/mL) were treated with 5 μM LL-37-FAM at 37 °C at the time points indicated, and imaged by confocal microscopy (scale bar indicated 10 μm). The MFI of LL-37-FAM in the endosomes is shown on the right. The results are representative of three independent experiments.

on monocytes, receptor down-regulation analysis after LL-37 treatment was performed. Since we have already reported on the lack of down regulation of FPR2 and P2X7 to LL-37 treated monocytes (Zhang et al., 2009), we only examined the possible roles of P2Y11, MRGX2, IGF1R, EGFR and Mac-1. As shown in Fig. 2A, MGRX2, P2Y11 and IGF1R were not detected on human monocytes as determined by flow cytometric analysis, ruling them out as candidates. While EGFR, CD11b, CD18 and CD115 (M-CSFR) were detected, only CXCR2 displayed down-regulation after LL-37-FAM treatment (Fig. 2A). Thus, similar to human neutrophils, CXCR2 is a major receptor for LL-37 on human monocytes.

To examine the co-localization of CXCR2 with LL-37, cells were treated with LL-37-FAM for 2 h and stained with antibodies to CXCR2 or with antibodies to CCR2 and CXCR4 as controls. As shown in Fig. 2B–D, both CCR2 and CXCR4 remain on the cell surface with little or no co-localization to cytosolic LL-37-FAM. Notably, a few cells (1 out of 25) exhibited co-localization of CCR2 with LL-37-FAM, while only CXCR2 exhibited consistent co-localization with LL-37, similar to LL-37 treated human neutrophils (Zhang et al., 2009). Interestingly, only a subset of internalized CXCR2 co-localized with LL-37-FAM, suggesting that while LL-37 triggers large-scale internalization of all cell surface CXCR2, only a portion of internalized CXCR2 remains associated with LL-37-FAM. While the mechanism behind this observation is unclear, differential endosomal sorting is likely.

Importantly, the portion of CXCR2 positive endosomes co-localized with LL-37-FAM remained at the later 4 and 16 h time points (Fig. S2). In addition, no re-expression of cell surface CXCR2 was found at these time points, demonstrating that recycling or re-synthesis of CXCR2 did not occur over 16 h. Since it was previously reported by our group that SB225002, a selective non-peptide CXCR2 antagonist, blocked LL-37-induced monocyte migration (Zhang et al., 2009), it is likely that CXCR2 plays a critical role in the response of monocytes to LL-37. We conclude that CXCR2 is the major receptor for LL-37 in human monocytes.

3.3. LL-37 is endocytosed by clathrin-dependent and caveolae/lipid raft-dependent pathways

Since it was reported that CXCR2 undergoes clathrin-mediated

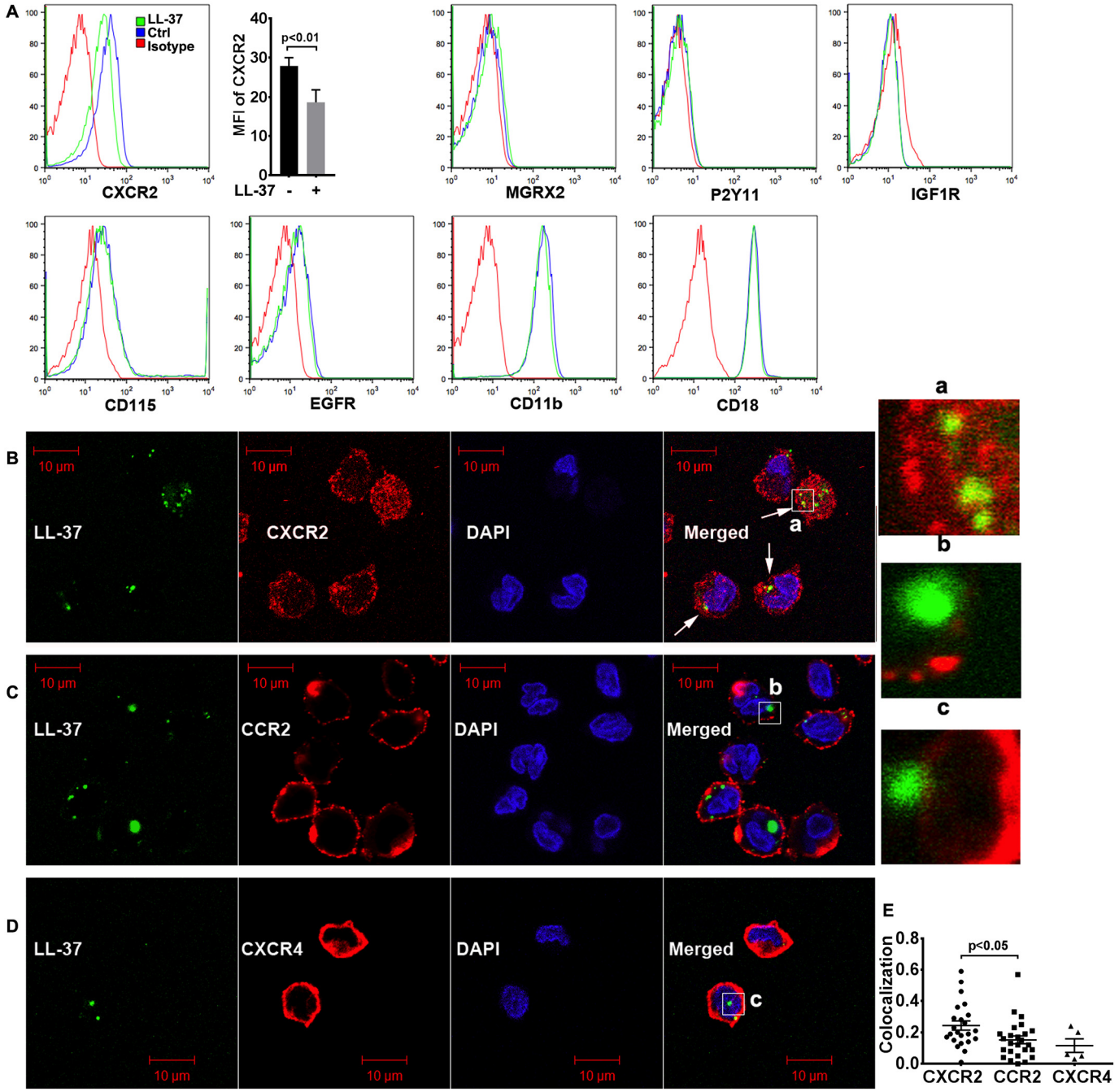

Fig. 2. LL-37 and CXCR2 are internalized and partially co-localized in the cytosol of human monocytes. (A) Human monocytes treated with 5 μM LL-37 for 2 h were stained with anti-CXCR2, anti-MRGX2, anti-P2Y11, anti-IGF1R, anti-EGFR, anti-CD18, anti-CD11b or anti-CD115 with isotype antibodies, and analyzed by flow cytometry. MFI of CXCR2 is shown on the right (n = 3). (B–D) Human monocytes (1×10^6 cells/mL) treated with 5 μM LL-37-FAM for 2 h as in Fig. 1, were stained with DAPI and anti-CXCR2 antibody, anti-CCR2 antibody or anti-CXCR4 antibody following detection with Alexa 555-conjugated secondary goat anti-mouse and imaged using confocal microscopy (scale bar 10 μm). Insets show magnified boxed areas (a–c). (E) Quantification of colocalization of LL-37-FAM with CXCR2, CCR2 or CXCR4 was analyzed using the Pearson correlation coefficient.

uptake after treatment of CXCR2 transfected HEK cells with CXCL8 (Yang et al., 1999), we considered the possibility that the uptake of LL-37/CXCR2 was also clathrin mediated. However, this does not rule out the alternative caveolae mediated pathway for LL-37 (Sigismund et al., 2005). Therefore, we co-stained LL-37-FAM treated monocytes with anti-clathrin heavy chain antibody as a marker for the clathrin-mediated pathway and anti-caveolin-1 antibody as marker for the caveolin-mediated pathway. At the 2 and 4 h time points, LL-37-FAM co-localized with clathrin heavy chain (Fig. 3A) and caveolin-1 (Fig. 3B), but not at the 16 h time point (images not shown). Quantitation of co-localization using Pearson correlation coefficient analysis is significant for both pathways (Fig. 3C).

To verify the role of the clathrin-dependent endocytosis, monocytes were pre-treated with Pitstop2, a selective cell-permeable clathrin inhibitor. As shown in Fig. 3D, Pitstop2 inhibited endocytosis of LL-37-FAM in a dose dependent manner. On the other hand, when monocytes were pretreated with nystatin, a caveolae-mediated endocytosis inhibitor (over the range of 6.25, 12.5, 25 and 50 μg/mL), endocytosis of LL-37-FAM was slightly increased (data not shown), a result in contrast to the previously reported results for THP-1 differentiated macrophages

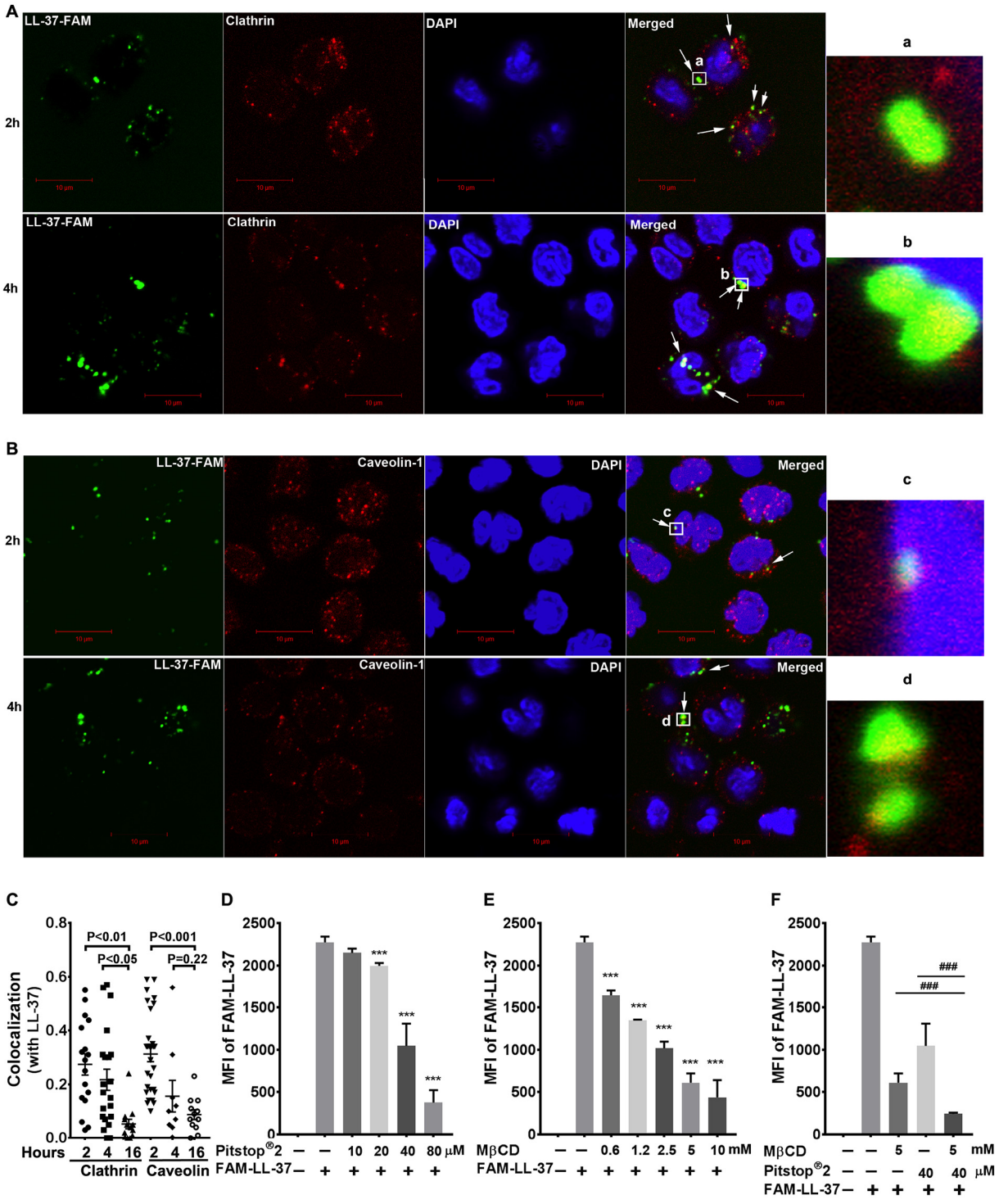

Fig. 3. LL-37 is internalized through clathrin- and caveolin-mediated pathways and is associated with lipid rafts. (A-B) Human monocytes (1×10^6 cells/mL) treated with 5 μM LL-37-FAM for 2 or 4 h were stained with DAPI and anti-clathrin heavy chain rabbit mAb or anti-caveolin-1 rabbit mAb following Alexa 555-conjugated secondary goat anti-rabbit IgG antibody, then observed using confocal microscopy (scale bar 10 μm (images at 16 h time point not shown). (C) Quantification of colocalization of LL-37-FAM with clathrin or caveolin-1 over time was analyzed using the Pearson correlation coefficient. (D–F) Human monocytes were pretreated with Pitstop2 (D), Methyl-β-cyclodextran (E) or both (F) for 30 min, then treated with 5 μM LL-37-FAM for 2 h. Mean fluorescence intensity (MFI) of LL-37-FAM was analyzed with flow cytometry ($n = 3$, $^{***}p < .001$ in comparison with LL-37-FAM alone, ### p < .001). Insets show magnified boxed areas (a–d).

or human monocyte derived macrophages (HMDMs) treated with LL-37 (Tang et al., 2015). To further investigate this apparent difference, monocytes were pre-treated with methyl-β-cyclodextrin (MβCD), a treatment that depletes cholesterol from lipid raft domains of plasma membranes enriched in caveolin (Zidovetzki and Levitan, 2007). As shown in Fig. 3E, MβCD suppressed endocytosis of LL-37-FAM of live monocytes (gated on live cells, Fig. S3A) in a dose dependent manner. Thus, lipid rafts play an important role in LL-37-FAM endocytosis, a result not unexpected since CXCR2, like all GPCRs, resides in the lipid raft rich domains. In fact, It was reported that GPCRs can be internalized by both caveolae-lipid raft and planar lipid raft pathways (Allen et al., 2007). The combination of treatments, 40 μM Pitstope2 and

5 mM MβCD, resulted in > 90% inhibition of LL-37-FAM endocytosis (Fig. 3F). Moreover, to explore if MβCD disrupted the surface expression of CXCR2, monocytes were treated with 5 mM MβCD only for 2.5 h and the expression level of CXCR2 was analyzed by flow cytometric analysis. Our results show that MβCD decreased the CXCR2 expression to a certain degree (Fig. S3B). Thus, we conclude that both clathrin- and caveolin/lipid rafts-mediated endocytosis are major pathways involving internalization of CXCR2 in response to LL-37.

Since the cationic amphiphilic peptide LL-37 is well known to be membrane active, binding to negatively charged lipids on plasma membranes (Kuroda et al., 2015), it is likely that lipid binding also plays a role. When monocytes were stained with the lipophilic dye FM 4–64 (Tamilselvam and Daefler, 2008) prior to treatment with LL-37-FAM and its membrane localization monitored over time, the results are consistent with the idea that LL-37-FAM remains associated with components of the plasma membrane (Fig. S4).

3.4. Rab5, APPL1 and EEA1 co-localize with LL-37-FAM in early endosomes

Rab5, a marker of early endosomes, plays an important role in both clathrin-mediated and clathrin-independent endocytosis (Mayor and Pagano, 2007; Le Roy and Wrana, 2005). Therefore, we co-stained LL-37-FAM vesicles for Rab5 at the 2–4 h time points (Fig. 4). Although we found that the LL-37-FAM and Rab5 were partially co-localized in endosomes over the time period 2–4 h, statistically, the results were not significant over the time course of treatment (Fig. 4A and D).

Since early endosomes contain either APPL (adaptor protein, phosphotyrosine interaction, PH domain, and leucine zipper-containing) or EEA1 (early endosomal antigen 1) adaptor proteins in addition to Rab5, further co-staining was performed. However, the presence of APPL1 or EEA1 in early endosomes is usually mutually exclusive since both of these adaptors bind to Rab5, competing for the same binding site (Wang et al., 2010). Not unexpectedly, LL-37-FAM predominantly co-localized with APPL1 at the 2 h time point (Fig. 4B and E) and with EEA1 at both the 2 and 4 h time points (Fig. 4C and F). Unlike Rab 5, the results for both markers are statistically significant over the time course of treatment. The lack of significance for Rab5 can be explained by its role in multiple endocytotic processes, while the markers APPL1 and EEA1 may be more dedicated to endocytosis of LL-37-FAM. Our results suggest that Rab5+ associated markers APPL1 and EEA1 are involved in the endocytosis of LL-37 and that segregation of the endosomes occurs through association first with APPL1 and then with EEA1.

3.5. Association of LL-37 with Rab9 and syntaxin-6 indicates uptake into the trans-Golgi network (TGN)

Following a stint in the early Rab5 positive early endosomal compartment, endosomes move into either Rab11 positive recycling endosomes or into late endosomes (Stenmark, 2009). Our analysis revealed that some LL-37-FAM positive endosomes co-localized with Rab11, but like Rab5, the results are not statistically significant over the time course of treatment (Fig. 5A and D). This result suggests that only a small percentage of endocytosed LL-37-FAM may be recycled. The fate of the remainder was analyzed by staining for syntaxin-6 and Rab9, markers for vesicular trafficking from early endosomes to the trans-Golgi network (TGN), a process that involves cargo-specific coat assembly of the late endosomes (Stenmark, 2009; Ganley et al., 2008). At the 2 h and 4 h time points, both syntaxin-6 and Rab9 positive vesicles partially co-localized with LL-37-FAM (Fig. 5B–C and E–F) in comparison with the 16 h time point.

3.6. The TGN and the mitochondria are destinations of endocytosed LL-37 vesicles

To determine the destination of endocytosed LL-37 vesicles in the cytosol, organelle staining of the TGN, mitochondria, lysosome and endoplasmic reticulum (ER) was performed. At the 4 h time point, Rhodamine-labeled LL-37 was partially co-localized with TGN co-stained with GOLGI-ID Green (Fig. 6A), a result in accordance with syntaxin-6 and Rab9 staining (Fig. 5B and C). At the 16 h time point, large Rhodamine-LL-37 positive vesicles remain co-localized with GOLGI-ID Green (Fig. 6A). At either the 4 or 16 h time points, we did not observe significant co-localization of endocytosed LL-37-FAM with the endoplasmic reticulum (ER) stained with ER-ID Red (Fig. S5A). In addition, a portion of endocytosed LL-37-FAM co-localized with lysosomes stained with LYSO-ID Red at 4 h and 16 h time point (Fig. S5B). Interestingly, LL-37-FAM partially co-localized with MITO-ID Red at both 4 and 16 h time points, suggesting that some LL-37-FAM positive endosomes were associated with mitochondria (Fig. 6B). To confirm the co-localization of LL-37 with mitochondria, immuno-EM was performed using gold-labeled antibodies to LL-37 at 21 h post LL-37 treatment (Fig. 6C). It can be seen that multiple mitochondria surround a large LL-37 positive vesicle with one to two mitochondria included in the vesicle and that gold staining surrounds the mitochondria in the vesicle. This finding is especially intriguing, since mitochondria co-localization with calcium rich vesicles was identified as specific sites of calcium phosphate mineralization in osteoblasts (Boonrungsiman et al., 2012). Given the fact that LL-37-treated monocytes differentiate into a novel type of bone forming cell (the monoosteophil) that accelerate bone repair in an animal model (Zhang and Shively, 2010; Zhang and Shively, 2013), the mitochondrial connection emphasizes their functional similarity to the osteoblast. Furthermore, the observation that endocytosed LL-37 in monocytes transits to both the mitochondria (Fig. 6C) and Golgi (Fig. 6D), connects these two sites as essential for monoosteophil differentiation. However, it should be emphasized that the osteoblasts are of mesenchymal stem cell origin (Chen et al., 2016) while monocytes are of hematopoietic stem cell origin. Thus, the two types of cells have distinct origins, emphasizing their different roles in primary bone mineralization or repair.

3.7. Formation of large LL-37 positive vesicles in 6-day LL-37-treated monocytes

Although we showed that LL-37-FAM, like unlabeled LL-37, reliably differentiates monocytes into monoosteophils (Fig. S1), it was important to determine if the observed signals for LL-37-FAM over time were associated with intact LL-37 or a fluorescent breakdown product. Therefore, monocytes treated with LL-37-FAM for 6 days were sectioned for EM and stained with an anti-LL-37 antibody followed by secondary antibody conjugated with 15 nm nanogold particles (Fig. 7). Immuno-EM reveals that the LL-37 peptide remains immunologically intact from 21 h (Fig. 6C) to the 6 day differentiation period (Fig. 7). Interestingly, the fine detail of the vesicle exhibits both granular and membranous inclusions. Taken together these results confirm that our observations are not artifacts of metabolism of LL-37-FAM vs LL-37.

Since the size of the LL-37-FAM positive vesicles was large (> 10 μm), it was important to determine their size distribution and location within the cytoplasm. As shown in Fig. 8, confocal 1 μm z-sections of a single monoosteophil reveals several LL-37-FAM positive structures in the cell, the larger of which is 10 × 2 μm in size, and the smaller about 6 × 2 μm. Thus, the size of LL-37-FAM positive vesicles is variable.

To determine if the 6 day LL-37-FAM positive vesicles were associated with other cellular organelles, the monoosteophils were co-stained for Golgi, mitochondria, lysosome and ER dyes (Fig. 9). The results demonstrate that LL-37-FAM positive structures are not associated with any of these organelles even though they were transiently

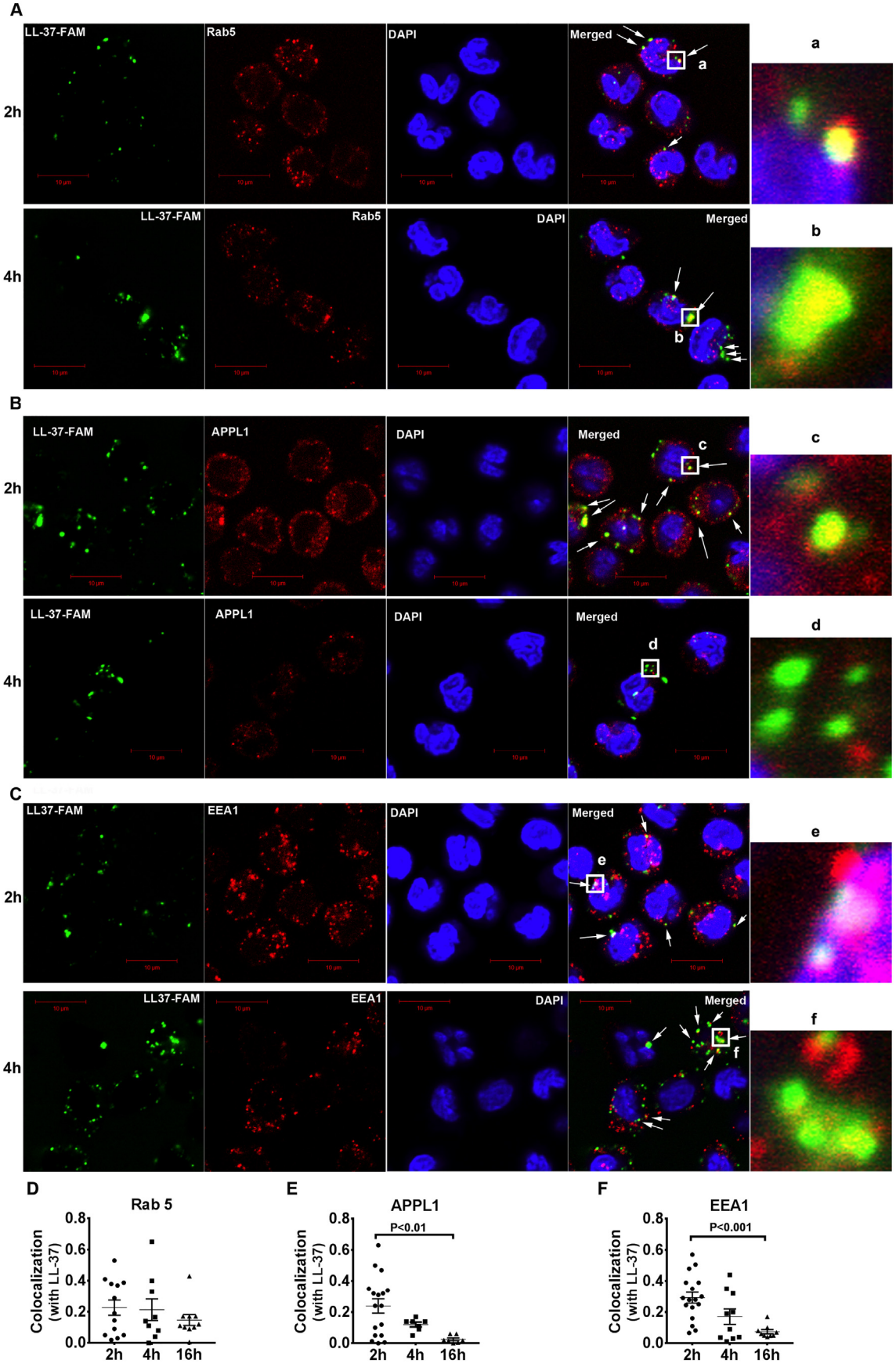

Fig. 4. Rab5, APPL1 and EEA1 are associated with LL-37 in early endosomes. Human monocytes (1×10^6 cells/mL) treated with 5 μM LL-37-FAM for 2, 4 or 16 h were stained with DAPI and Rab5 rabbit mAb (A), anti-APPLI rabbit mAb (B), EEA1 rabbit mAb (C), following with Alexa 555-conjugated secondary goat anti-rabbit IgG antibody, then observed using confocal microscopy (scale bar 10 μm (images at 16 h time point not shown). Insets show magnified boxed areas (a–f). Quantification of colocalization of LL-37-FAM with Rab5 (D), APPL1 (E) or EEA1 (F) over time was analyzed using the Pearson correlation coefficient.

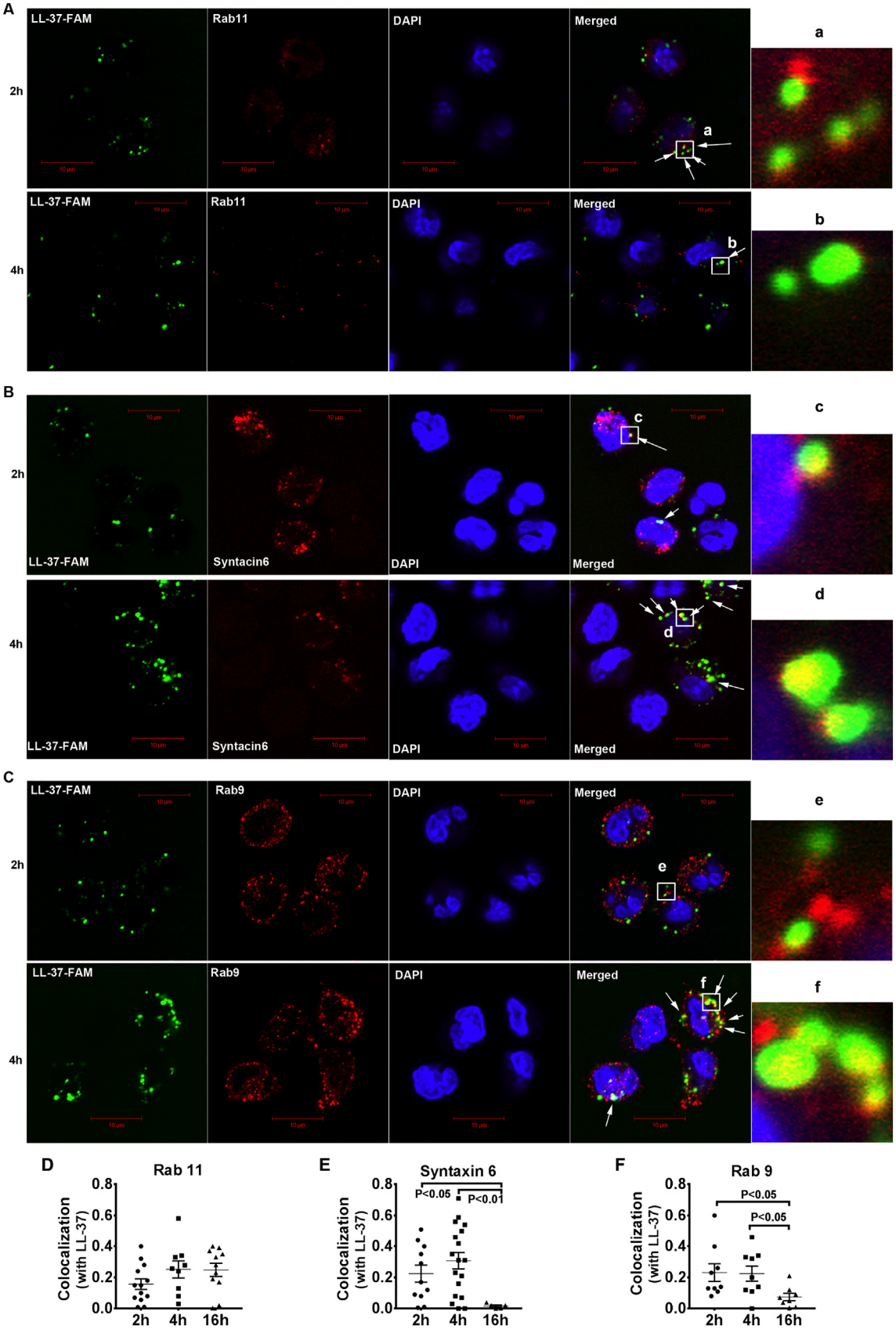

Fig. 5. Rab11, Syntaxin-6 and Rab9 co-localize with endocytosed LL-37 vesicles. Human monocytes treated with 5 μM FAM-labeled LL-37 for 2, 4 or 16 h were stained with DAPI and anti-Rab11 (D4F5) rabbit mAb (A), anti-Syntaxin-6 rabbit mAb (B), or anti-Rab9A rabbit mAb (C), following with Alexa 555-conjugated secondary goat anti-rabbit IgG antibody, then observed using confocal microscopy (scale bar 10 μm, images in 16 h time point not shown). Insets show magnified boxed areas (a-f). Quantification of colocalization of LL-37-FAM with Rab11 (D), Syntaxin-6 (E) or Rab9 (F) over time was analyzed using the Pearson correlation coefficient.

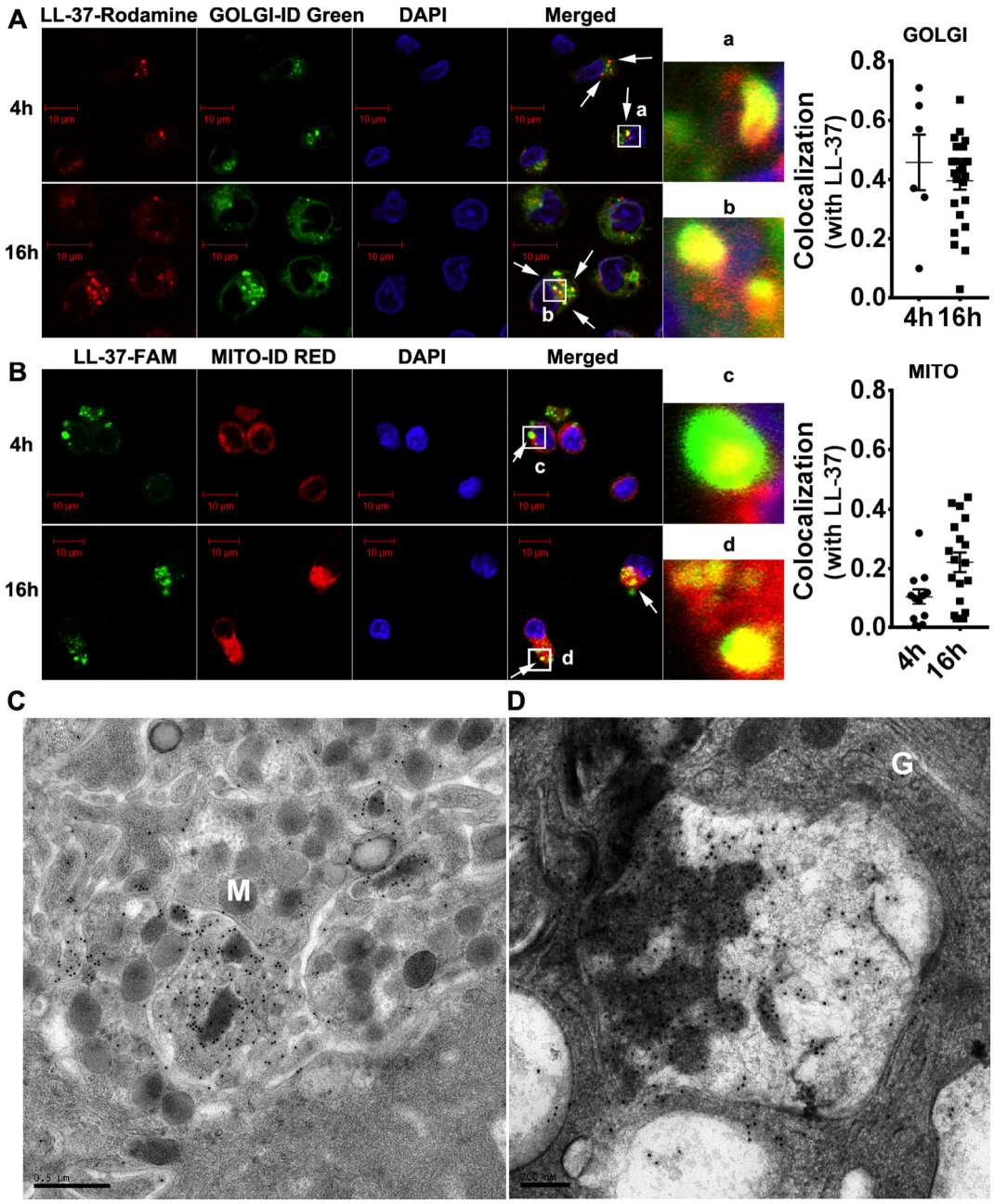

Fig. 6. Golgi and mitochondria are associated with endocytosed LL-37 vesicles. Human monocytes treated with 5 μM Rhodamine-LL-37 (A) or LL-37-FAM (B) for 4 or 16 h were stained with GOLGI-ID Green (A) or MITO-ID Red (B). The association of LL-37 with Golgi (A) or Mitochondria (B) was observed using confocal microscopy (scale bar 10 μm). Quantification of LL-37-FAM with GOLGI-ID Green or MITO-ID RED over time was analyzed using the Pearson correlation coefficient as shown at the right. (C) LL-37 treated monocytes (21h) were analyzed by immune-EM using nanogold labeled anti-LL-37 antibody. The figure shows a section where antibody staining was detected within a membrane defined vesicle surrounded by mitochondria (M) including two mitochondria within the vesicle (scale bar 0.5 μm). (D) Another immuno-EM stained section (scale bar 0.5 μm) showing a gold labeled vesicle adjacent to the TGN (G). The figures of immune-EM are the representatives of ten cells.

associated with the Golgi and Mitochondria at the 4 h and 16 h time points (Fig. 6A and B). The results suggest a sequential maturation of the LL-37-FAM labeled vesicles into unique, large vesicles. The fact that LL-37 remains embedded within vesicles during the entire process is striking, suggesting that it plays a critical role in directing the maturation process throughout the 6 day observation period and that it is not metabolically degraded.

3.8. Characteristics of large LL-37 vesicles

Since our previous study identified a unique gene profile associated with the differentiation of monocytes into monoosteophils (Zhang and Shively, 2013), we analyzed the cell membranes of the large LL-37 vesicles for protein expression of several of the genes identified. Indeed, large LL-37 vesicles membranes were strongly positive for integrin α3 (CD49c), CD9, CD59 and CD276 (Fig. 10). Previously, we showed that integrin α3β1, also known as very late (activation) antigen 3 (VLA3), was part of a unique set of markers for monoosteophils, namely $CD45^{+}\alpha3^{+}\alpha3\beta1^{+}CD34^{-}CD14^{-}BAP^{-}$ (bone alkaline phosphatase) cells (Zhang and Shively, 2013). Importantly, integrin α3 was also found on the large LL-37 vesicles (Fig. 10A). Since monoosteophils begin to express integrin α3 at day 1, followed by a significant increase

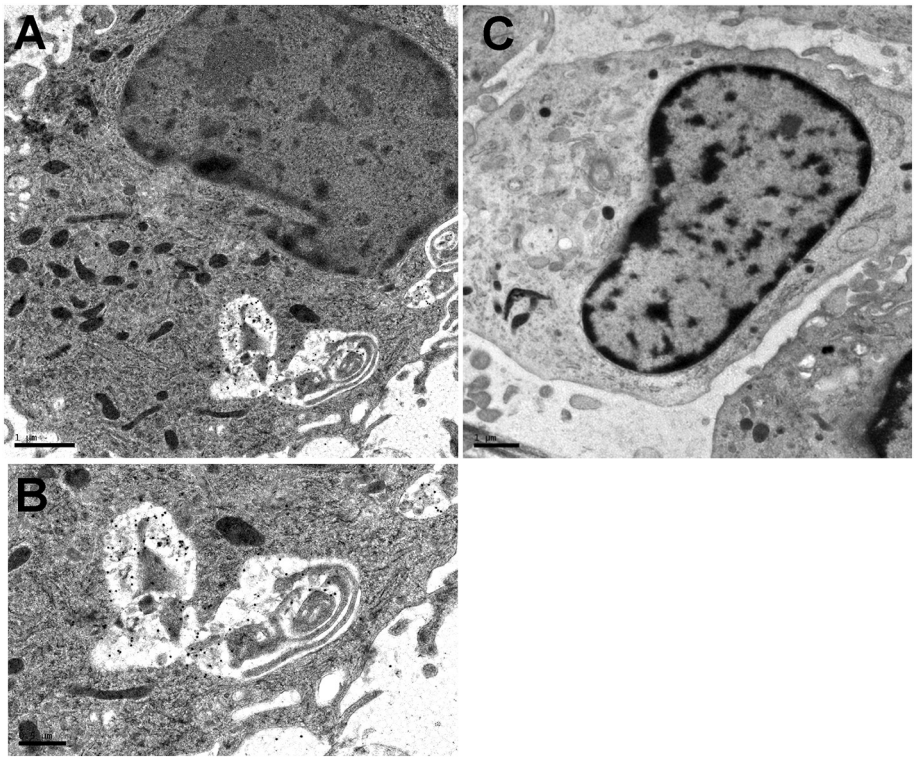

Fig. 7. Immuno-EM and confocal microscopy analysis of large LL-37 vesicles. Human monocytes treated with 5 μM LL-37-FAM for 6 days plus 2 days with $CaCl_2$ were visualized using anti-LL-37 antibody following by 15 nm gold labeled goat anti-mouse IgG antibody by immuno-EM. A: bar = 1 μm. B: bar = 0.5 μm. C: Monocyte control not treated with LL37, followed by 15 nm gold labeled goat anti-mouse IgG antibody by immuno-EM.

by day 3 (Zhang and Shively, 2013), it is likely that newly synthesized integrin α3 in the TGN is delivered to the monoosteosomes that transit to both the TGN and mitochondria.

CD9, a member of the tetraspanin family, is a cell surface glycoprotein that is known to complex with integrins and other TM4 superfamily proteins (Hemler, 2005). CD9 is found on the surface of exosomes (Lai et al., 2010) and plays a critical role in events such as sperm–egg fusion (Rubinstein et al., 2006). CD9 is expressed on the cell surface of monoosteophils and is co-localized to large LL-37 vesicles (Fig. 10B). CD59 is a glycophosphatidylinositol (GPI) anchored cell surface protein that is involved in functions including endocytosis of the CD59-CD9 complex (Maio et al., 1998). CD59 also co-localizes with large LL-37 vesicles and is expressed on the cell surface of monoosteophils (Fig. 10C).

CD276, or B7-H3, is an important immune checkpoint member of the B7 and CD28 families that regulates both innate and adaptive immunity during homeostasis and inflammation (Picarda et al., 2016). Beyond the immune system, the B7-H3 pathway has a non-immunologic role in promoting osteoblast differentiation and bone mineralization in mice, ensuring normal bone formation (Suh et al., 2004). As shown in Fig. 10D, monoosteophils are CD276 positive cells with CD276 co-localized to large LL-37 vesicles. For comparison, the cell surface staining of fresh monocytes, 6 day cultured macrophages and 6 day monoosteophils for integrin α3, CD9, CD59 and CD276 are shown in Fig. S6. We hypothesize that each of these monoosteophil membrane markers play an important role in their bone repair function.

4. Conclusion

While bone turnover is well understood from the point of view of degradation by osteoclasts and renewal by osteoblasts (Naylor and Eastell, 2012), the process of bone repair after injury is less understood. It has been hypothesized that circulating cells of different origin(s) play a role in bone repair, besides the bone marrow resident cells that include osteoblasts and osteoclasts (Fadini et al., 2012). It should not be unexpected that inflammation plays a major role in initiating the bone repair process and that circulating monocytes may migrate to the site of injury, especially if the injury includes the introduction of bacteria. In this respect, we hypothesize that anti-bacterial mediators of inflammation, like LL-37 would be present at the site of injury and activate migrating monocytes to perform tasks such as repair of the injury. In this way, we identified monoosteophils, a unique LL-37 differentiated cell type, that expressed markers of both the osteoblast and osteoclast lineage (Zhang and Shively, 2010; Zhang and Shively, 2013), that built mineralized calcium phosphate in vitro and accelerated bone repair in a NOD/SCID mouse model (Zhang and Shively, 2013). Moreover, monoosteophils are also predicted to play an important role in bone turnover (Fadini et al., 2012). In accordance with our report, Fadini and coworkers reported that myeloid calcifying OC^+BAP^+ cells (MCCs) could be differentiated from monocytes of peripheral blood mononuclear cells, and generation of MCCs was closely associated with expression of the osteogenic transcription factor Runx2 and high glucose increased calcification by MCCs in vitro (Fadini et al., 2011).

Although we previously determined the gene signature and function of monoosteophils, we did not explore the mechanism of uptake of LL-37. We have now shown that CXCR2 is the major receptor of LL-37 in human monocytes as evidenced by its down-regulation from the monocyte surface and its colocalization with endocytosed LL-37. This, together with our report that SB225002, a selective non-peptide CXCR2 antagonist, blocked LL-37-induced monocyte migration (Zhang et al., 2009) solidifies a critical role for a LL-37-CXCR2 axis in monocytes. Given the fact that GROα, a CXCR2 agonist, was not able to induce monocyte differentiation into monoosteophils (data not shown), we conclude that the LL-37/CXCR2 mediated formation of monoosteophils is distinct from other CXCR2 mediated functions. In support of this idea, LL-37 induces a unique pattern of prolonged calcium mobilization compared to GROα- or CXCL8-induced transient calcium mobilization (De et al., 2000; Zhang et al., 2009). This is important, since calcium is one of the two main sources of mineralization in these cells, the other being inorganic phosphate. The fact that LL-37 is a membrane active agent and binds to the lipid raft associated GPCR CXCR2 may be important. In agreement with this idea, we showed that cholesterol depletion reagent, MβCD, suppressed endocytosis of LL-37-FAM in a dose dependent manner, suggesting that the lipid raft itself may play a role

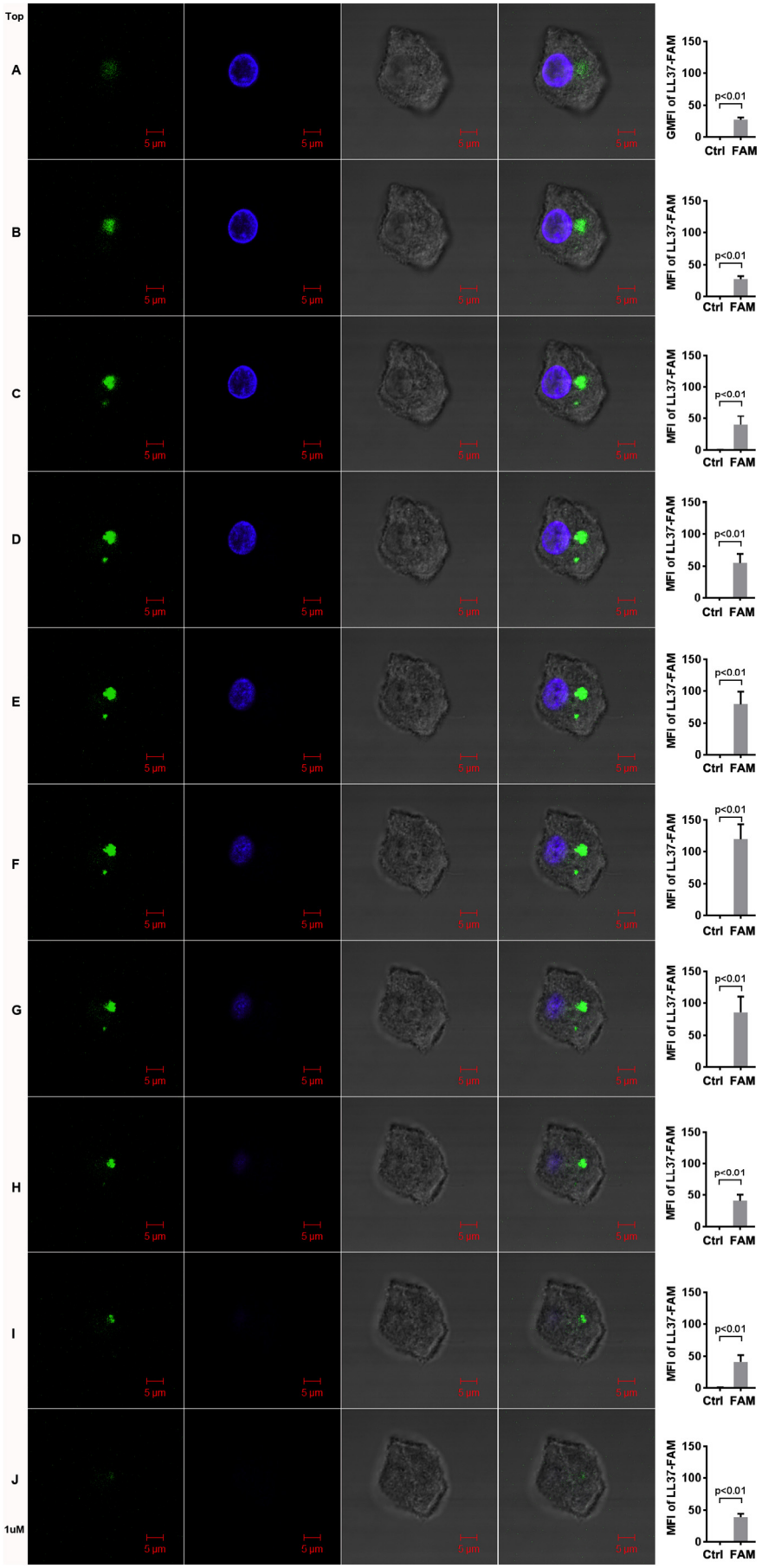

(caption on next page)

Fig. 8. Large LL-37 vesicle dimensions in 6 day differentiated large LL-37 vesicles. Human monocytes treated with 5 μM LL-37-FAM for 6 days were observed by confocal microscopy using z-section analysis (1 μm/section, scale bar 5 μm). MFI of LL-37-FAM is shown on the right. The figures are representative of three independent experiments.

in LL-37 signaling. In accordance with previous studies on CXCR2 mediated internalization (Fan et al., 2003), we also found that the clathrin- and caveolin/lipid raft-dependent pathways, as well as Rab5, APPL1 and EEA1 are involved with LL-37/CXCR2 internalization.

Surprisingly, LL-37 remains associated with the membrane of the internalized endosomes during the complex process of transition from early to late endosomes, including formation of the large LL-37 positive vesicles. Not unexpectedly, the early endosomes transit to several locations, including the TGN, and mitochondria, likely picking up critical components required for subsequent mineralization. In the case of the TGN newly synthesized proteins can contribute to the process, and in the case of the mitochondria, access to calcium and inorganic phosphate may contribute to mineralization, similar to that observed for the osteoblast (Boonrungsiman et al., 2012). After six days, the process results in a very large structure that includes many of the unique gene signature proteins we previously identified by our gene chip analysis (Zhang and Shively, 2013). Thus, LL-37, a multi-functional peptide that combines anti-bacterial activities as well as activation of innate immunity, is now shown to play a role in the generation of a new mineralization structure during the differentiation of monocytes into monoosteophils. Although much remains to be studied in the detailed mechanism of this process, we believe that this analysis will provoke further work on the pleotropic nature of monocytes that play important roles in cell biology, the immune system and tissue repair.

Author contributions

ZZ and JES conceived the experiments and wrote the paper. ZZ, BA, and MM analyzed results. ZZ, KL and DLP performed the experiments.

Transparency document

The Transparency document associated with this article can be found, in online version.

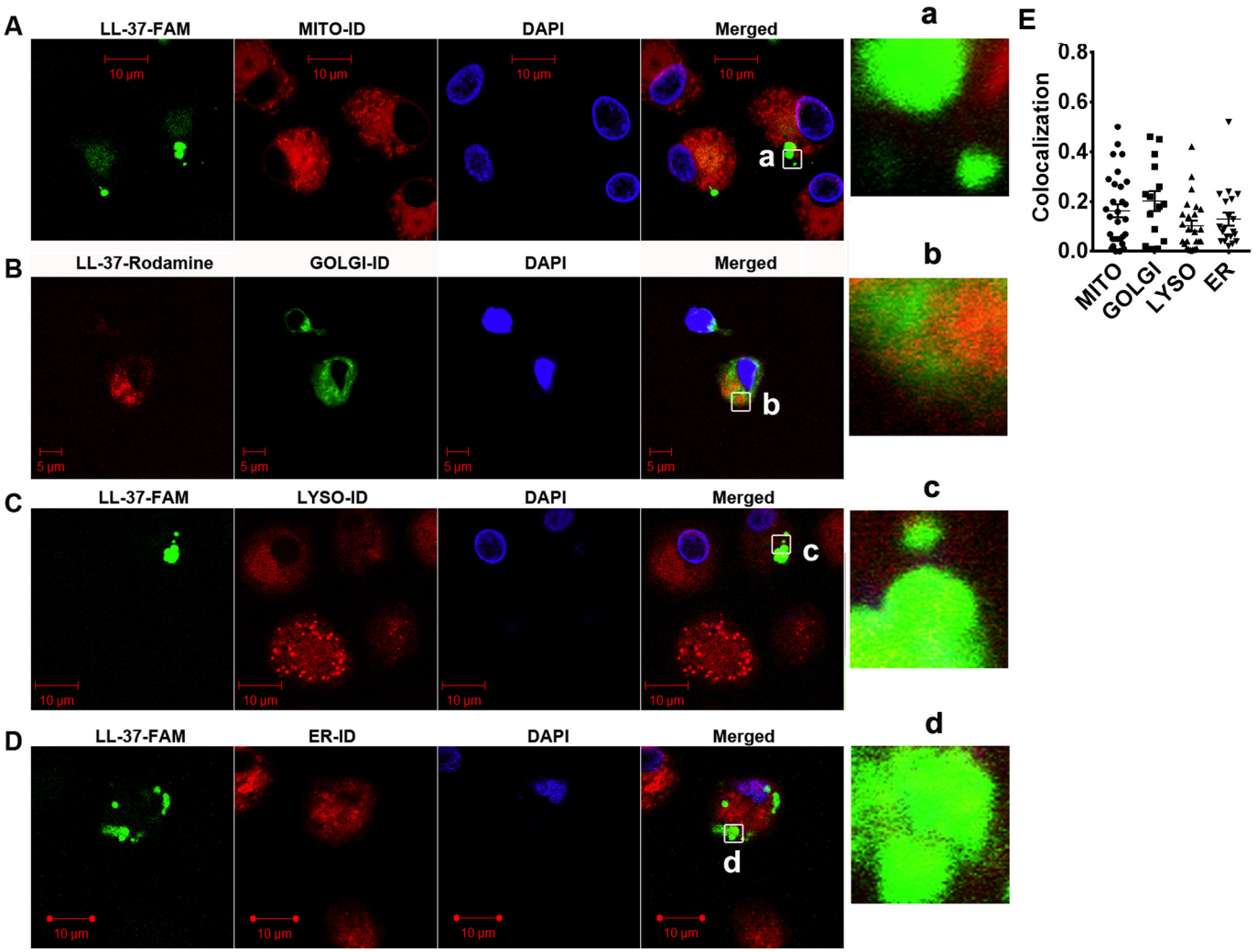

Fig. 9. Large LL-37 vesicles are distinct from Golgi, mitochondria, endoplastic reticulum (ER) and lysosomes. Human monocytes were treated with 5 μM LL-37-FAM (A, C, D) or Rhodamine-LL-37 (B) for 6 days. Cells were harvested, washed with PBS, fixed/permeabilized, stained with MITO-ID Red dye (A), GOLGI-ID Green dye (B), LYSO-ID Red dye (C) or ER-ID Red dye (D). Colocalization of LL-37 with above organelles (a–b). Quantification of colocalization of LL-37-FAM with above organelles was analyzed using the Pearson correlation coefficient (E).

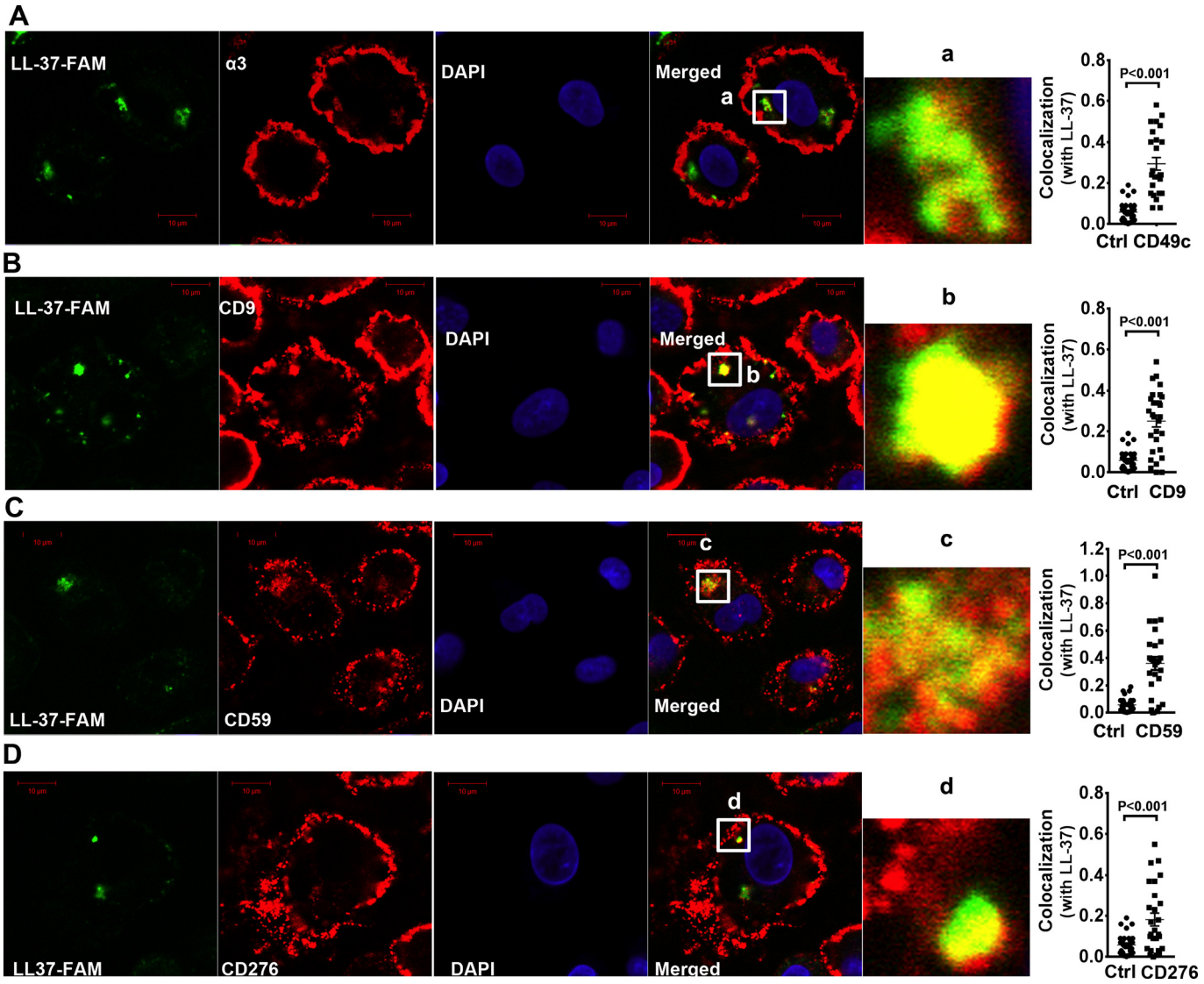

Fig. 10. Large LL-37 vesicles co-stain with integrin a3, CD9, CD59, and CD276. Human monocytes treated with 5 μM LL-37-FAM for 6 days were stained with anti-α3 integrin (CD49c) antibody (B), anti-CD9 antibody (C), anti-CD59 antibody (D), or anti-CD276 antibody (E) following by Alexa555 conjugated goat anti-mouse IgG antibody, and observed using confocal microscopy. Quantification of colocalization of LL-37-FAM with CD49c, CD9, CD59 or CD276 was analyzed by the Pearson correlation coefficient. Control (Ctrl) represents the quantification of colocalization of LL-37-FAM with TIMP3, an upregulated mRNA of genes in monoosteophils.

Declaration of competing interest

The authors declare no conflict of interest.

Acknowledgements

This research was supported in part by the City of Hope Comprehensive Cancer Center Grant CA033572. The authors thank Loren Quintanar in the Light Microscopy core for assisting confocal microscopy and Ricardo Zerda Noriega and Dr. Zhuo Li in the Electron Microscopy Core for immune-electron microscopy.

Appendix A. Supplementary data

Supplementary data to this article can be found online at https://doi.org/10.1016/j.bonr.2019.100237.

References

Agerberth, B., Charo, J., Werr, J., Olsson, B., Idali, F., Lindbom, L., Kiessling, R., Jornvall, H., Wigzell, H., Gudmundsson, G.H., 2000. The human antimicrobial and chemotactic peptides LL-37 and alpha-defensins are expressed by specific lymphocyte and monocyte populations. Blood 96 (9), 3086–3093.

Allen, J.A., Halverson-Tamboli, R.A., Rasenick, M.M., 2007. Lipid raft microdomains and neurotransmitter signalling. Nat. Rev. Neurosci. 8 (2), 128–140.

Bandholtz, L., Ekman, G.J., Vilhelmsson, M., Buentke, E., Agerberth, B., Scheynius, A., Gudmundsson, G.H., 2006. Antimicrobial peptide LL-37 internalized by immature human dendritic cells alters their phenotype. Scand. J. Immunol. 63 (6), 410–419.

Bjorstad, A., Askarieh, G., Brown, K.L., Christenson, K., Forsman, H., Onnheim, K., Li, H.N., Teneberg, S., Maier, O., Hoekstra, D., et al., 2009. The host defense peptide LL-37 selectively permeabilizes apoptotic leukocytes. Antimicrob. Agents Chemother. 53 (3), 1027–1038.

Boonrungsiman, S., Gentleman, E., Carzaniga, R., Evans, N.D., McComb, D.W., Porter, A.E., Stevens, M.M., 2012. The role of intracellular calcium phosphate in osteoblast-mediated bone apatite formation. Proc. Natl. Acad. Sci. U. S. A. 109 (35), 14170–14175.

Brandenburg, L.O., Jansen, S., Wruck, C.J., Lucius, R., Pufe, T., 2010. Antimicrobial peptide rCRAMP induced glial cell activation through P2Y receptor signalling pathways. Mol. Immunol. 47 (10), 1905–1913.

Chen, Q., Shou, P., Zheng, C., Jiang, M., Cao, G., Yang, Q., Cao, J., Xie, N., Velletri, T., Zhang, X., et al., 2016. Fate decision of mesenchymal stem cells: adipocytes or osteoblasts? Cell Death Differ. 23 (7), 1128–1139.

Chromek, M., Slamova, Z., Bergman, P., Kovacs, L., Podracka, L., Ehren, I., Hokfelt, T., Gudmundsson, G.H., Gallo, R.L., Agerberth, B., et al., 2006. The antimicrobial peptide cathelicidin protects the urinary tract against invasive bacterial infection. Nat. Med. 12 (6), 636–641.

De, Y., Chen, Q., Schmidt, A.P., Anderson, G.M., Wang, J.M., Wooters, J., Oppenheim, J.J., Chertov, O., 2000. LL-37, the neutrophil granule- and epithelial cell-derived cathelicidin, utilizes formyl peptide receptor-like 1 (FPRL1) as a receptor to chemoattract human peripheral blood neutrophils, monocytes, and T cells. J. Exp. Med. 192 (7), 1069–1074.

Elssner, A., Duncan, M., Gavrilin, M., Wewers, M.D., 2004. A novel P2X7 receptor activator, the human cathelicidin-derived peptide LL37, induces IL-1 beta processing and release. J. Immunol. 172 (8), 4987–4994.

Fadini, G.P., Albiero, M., Menegazzo, L., Boscaro, E., Vigili de Kreutzenberg, S., Agostini, C., Cabrelle, A., Binotto, G., Rattazzi, M., Bertacco, E., et al., 2011. Widespread increase in myeloid calcifying cells contributes to ectopic vascular calcification in type 2 diabetes. Circ. Res. 108 (9), 1112–1121.

Fadini, G.P., Rattazzi, M., Matsumoto, T., Asahara, T., Khosla, S., 2012. Emerging role of circulating calcifying cells in the bone-vascular axis. Circulation 125 (22), 2772–2781.

Fan, G.H., Lapierre, L.A., Goldenring, J.R., Richmond, A., 2003. Differential regulation of CXCR2 trafficking by Rab GTPases. Blood 101 (6), 2115–2124.

Ganley, I.G., Espinosa, E., Pfeffer, S.R., 2008. A syntaxin 10-SNARE complex distinguishes two distinct transport routes from endosomes to the trans-Golgi in human cells. J. Cell Biol. 180 (1), 159–172.

Girnita, A., Zheng, H., Gronberg, A., Girnita, L., Stahle, M., 2012. Identification of the cathelicidin peptide LL-37 as agonist for the type I insulin-like growth factor receptor. Oncogene 31 (3), 352–365.

Hancock, R.E., Haney, E.F., Gill, E.E., 2016. The immunology of host defence peptides: beyond antimicrobial activity. Nat Rev Immunol 16 (5), 321–334.

Heilborn, J.D., Nilsson, M.F., Kratz, G., Weber, G., Sorensen, O., Borregaard, N., Stahle-Backdahl, M., 2003. The cathelicidin anti-microbial peptide LL-37 is involved in re-epithelialization of human skin wounds and is lacking in chronic ulcer epithelium. The Journal of investigative dermatology 120 (3), 379–389.

Hemler, M.E., 2005. Tetraspanin functions and associated microdomains. Nat Rev Mol Cell Biol 6 (10), 801–811.

Hoppenbrouwers, T., Autar, A.S.A., Sultan, A.R., Abraham, T.E., van Cappellen, W.A., Houtsmuller, A.B., van Wamel, W.J.B., van Beusekom, H.M.M., van Neck, J.W., de Maat, M.P.M., 2017. In vitro induction of NETosis: comprehensive live imaging comparison and systematic review. PLoS One 12 (5), e0176472.

Koczulla, R., von Degenfeld, G., Kupatt, C., Krotz, F., Zahler, S., Gloe, T., Issbrucker, K., Unterberger, P., Zaiou, M., Lebherz, C., et al., 2003. An angiogenic role for the human peptide antibiotic LL-37/hCAP-18. J. Clin. Invest. 111 (11), 1665–1672.

Kuroda, K., Okumura, K., Isogai, H., Isogai, E., 2015. The human cathelicidin anti-microbial peptide LL-37 and mimics are potential anticancer drugs. Front. Oncol. 5, 144.

Lai, R.C., Arslan, F., Lee, M.M., Sze, N.S., Choo, A., Chen, T.S., Salto-Tellez, M., Timmers, L., Lee, C.N., El Oakley, R.M., et al., 2010. Exosome secreted by MSC reduces myocardial ischemia/reperfusion injury. Stem Cell Res. 4 (3), 214–222.

Le Roy, C., Wrana, J.L., 2005. Clathrin- and non-clathrin-mediated endocytic regulation of cell signalling. Nat Rev Mol Cell Biol 6 (2), 112–126.

Li, H.N., Barlow, P.G., Bylund, J., Mackellar, A., Bjorstad, A., Conlon, J., Hiemstra, P.S., Haslett, C., Gray, M., Simpson, A.J., et al., 2009. Secondary necrosis of apoptotic neutrophils induced by the human cathelicidin LL-37 is not proinflammatory to phagocytosing macrophages. J. Leukoc. Biol. 86 (4), 891–902.

Maio, M., Brasoveanu, L.I., Coral, S., Sigalotti, L., Lamaj, E., Gasparollo, A., Visintin, A., Altomonte, M., Fonsatti, E., 1998. Structure, distribution, and functional role of protectin (CD59) in complement-susceptibility and in immunotherapy of human malignancies (review). Int. J. Oncol. 13 (2), 305–318.

Mayor, S., Pagano, R.E., 2007. Pathways of clathrin-independent endocytosis. Nat Rev Mol Cell Biol 8 (8), 603–612.

Naylor, K., Eastell, R., 2012. Bone turnover markers: use in osteoporosis. Nat. Rev. Rheumatol. 8 (7), 379–389.

Picarda, E., Ohaegbulam, K.C., Zang, X., 2016. Molecular pathways: targeting B7-H3 (CD276) for human cancer immunotherapy. Clin. Cancer Res. 22 (14), 3425–3431.

Rivas-Santiago, B., Hernandez-Pando, R., Carranza, C., Juarez, E., Contreras, J.L., Aguilar-Leon, D., Torres, M., Sada, E., 2008. Expression of cathelicidin LL-37 during mycobacterium tuberculosis infection in human alveolar macrophages, monocytes, neutrophils, and epithelial cells. Infect. Immun. 76 (3), 935–941.

Rubinstein, E., Ziyyat, A., Wolf, J.P., Le Naour, F., Boucheix, C., 2006. The molecular players of sperm-egg fusion in mammals. Semin. Cell Dev. Biol. 17 (2), 254–263.

Scott, M.G., Davidson, D.J., Gold, M.R., Bowdish, D., Hancock, R.E., 2002. The human antimicrobial peptide LL-37 is a multifunctional modulator of innate immune responses. J. Immunol. 169 (7), 3883–3891.

Sigismund, S., Woelk, T., Puri, C., Maspero, E., Tacchetti, C., Transidico, P., Di Fiore, P.P., Polo, S., 2005. Clathrin-independent endocytosis of ubiquitinated cargos. Proc. Natl. Acad. Sci. U. S. A. 102 (8), 2760–2765.

Sigurdardottir, S.L., Thorleifsdottir, R.H., Guzman, A.M., Gudmundsson, G.H., Valdimarsson, H., Johnston, A., 2012. The anti-microbial peptide LL-37 modulates immune responses in the palatine tonsils where it is exclusively expressed by neutrophils and a subset of dendritic cells. Clin. Immunol. 142 (2), 139–149.

Sonawane, A., Santos, J.C., Mishra, B.B., Jena, P., Progida, C., Sorensen, O.E., Gallo, R., Appelberg, R., Griffiths, G., 2011. Cathelicidin is involved in the intracellular killing of mycobacteria in macrophages. Cell. Microbiol. 13 (10), 1601–1617.

Sorensen, O., Arnljots, K., Cowland, J.B., Bainton, D.F., Borregaard, N., 1997. The human antibacterial cathelicidin, hCAP-18, is synthesized in myelocytes and metamyelocytes and localized to specific granules in neutrophils. Blood 90 (7), 2796–2803.

Stenmark, H., 2009. Rab GTPases as coordinators of vesicle traffic. Nat Rev Mol Cell Biol 10 (8), 513–525.

Subramanian, H., Gupta, K., Guo, Q., Price, R., Ali, H., 2011. Mas-related gene X2 (MrgX2) is a novel G protein-coupled receptor for the antimicrobial peptide LL-37 in human mast cells: resistance to receptor phosphorylation, desensitization, and internalization. J. Biol. Chem. 286 (52), 44739–44749.

Suh, W.K., Wang, S.X., Jheon, A.H., Moreno, L., Yoshinaga, S.K., Ganss, B., Sodek, J., Grynpas, M.D., Mak, T.W., 2004. The immune regulatory protein B7-H3 promotes osteoblast differentiation and bone mineralization. Proc. Natl. Acad. Sci. U. S. A. 101 (35), 12969–12973.

Tamilselvam, B., Daefler, S., 2008. Francisella targets cholesterol-rich host cell membrane domains for entry into macrophages. J. Immunol. 180 (12), 8262–8271.

Tang, X., Basavarajappa, D., Haeggstrom, J.Z., Wan, M., 2015. P2X7 receptor regulates internalization of antimicrobial peptide LL-37 by human macrophages that promotes intracellular pathogen clearance. J. Immunol. 195 (3), 1191–1201.

Vandamme, D., Landuyt, B., Luyten, W., Schoofs, L., 2012. A comprehensive summary of LL-37, the factotum human cathelicidin peptide. Cell. Immunol. 280 (1), 22–35.

Wang, Y., Nakayama, M., Pitulescu, M.E., Schmidt, T.S., Bochenek, M.L., Sakakibara, A., Adams, S., Davy, A., Deutsch, U., Luthi, U., et al., 2010. Ephrin-B2 controls VEGF-induced angiogenesis and lymphangiogenesis. Nature 465 (7297), 483–486.

Yang, W., Wang, D., Richmond, A., 1999. Role of clathrin-mediated endocytosis in CXCR2 sequestration, resensitization, and signal transduction. J. Biol. Chem. 274 (16), 11328–11333.

Yang, D., Biragyn, A., Hoover, D.M., Lubkowski, J., Oppenheim, J.J., 2004. Multiple roles of antimicrobial defensins, cathelicidins, and eosinophil-derived neurotoxin in host defense. Annu. Rev. Immunol. 22, 181–215.

Yin, J., Yu, F.S., 2010. LL-37 via EGFR transactivation to promote high glucose-attenuated epithelial wound healing in organ-cultured corneas. Invest. Ophthalmol. Vis. Sci. 51 (4), 1891–1897.

Zhang, Z., Shively, J.E., 2010. Generation of novel bone forming cells (monoosteophils) from the cathelicidin-derived peptide LL-37 treated monocytes. PLoS One 5 (11), e13985.

Zhang, Z., Shively, J.E., 2013. Acceleration of bone repair in NOD/SCID mice by human monoosteophils, novel LL-37-activated monocytes. PLoS One 8 (7), e67649.

Zhang, Z., Cherryholmes, G., Shively, J.E., 2008. Neutrophil secondary necrosis is induced by LL-37 derived from cathelicidin. J. Leukoc. Biol. 84 (3), 780–788.

Zhang, Z., Cherryholmes, G., Chang, F., Rose, D.M., Schraufstatter, I., Shively, J.E., 2009. Evidence that cathelicidin peptide LL-37 may act as a functional ligand for CXCR2 on human neutrophils. Eur. J. Immunol. 39 (11), 3181–3194.

Zhang, X., Bajic, G., Andersen, G.R., Christiansen, S.H., Vorup-Jensen, T., 2016. The cationic peptide LL-37 binds mac-1 (CD11b/CD18) with a low dissociation rate and promotes phagocytosis. Biochim. Biophys. Acta 1864 (5), 471–478.

Zidovetzki, R., Levitan, I., 2007. Use of cyclodextrins to manipulate plasma membrane cholesterol content: evidence, misconceptions and control strategies. Biochim. Biophys. Acta 1768 (6), 1311–1324.